Observed Subseasonal Variability of Oceanic Barrier and Compensated Layers

HAILONG LIU, SEMYON A. GRODSKY, AND JAMES A. CARTON

Department of Atmospheric and Oceanic Science, University of Maryland, College Park, College Park, Maryland

(Manuscript received 11 December 2008, in final form 10 June 2009)

ABSTRACT

A monthly gridded analysis of barrier-layer and compensated-layer width based on observed vertical profiles of temperature and salinity and covering the period 1960–2007 is explored for evidence of subseasonal variability and its causes. In the subtropics and midlatitudes this variability is mostly evident during the local cold season when barrier layers and compensated layers are present. There is significant variability of anomalous (nonseasonal) barrier-layer and compensated-layer width on interannual periods, while in the North Pacific longer-term changes are also detectable. In the winter North Pacific a salinity-stratified barrier layer exists at subpolar latitudes. Farther south along the Kuroshio Extension a compensated layer exists. The width of the barrier layer varies from year to year by up to 60 m while compensated-layer width varies by half as much. During the observation period the barrier-layer width decreased in response to a strengthening of the Aleutian low pressure system, the resulting strengthening of dry northerly winds, and a decrease of precipitation. In contrast, the compensated-layer width increased in response to this pressure system strengthening and related amplification of the midlatitude westerly winds, the resulting increase of net surface heat loss, and its effect on the temperature and salinity of the upper-ocean water masses. The tropical Pacific, Atlantic, and Indian Oceans all have permanent barrier layers. Their interannual variability is less than 20 m but is comparable in magnitude to the time mean barrier-layer width in these areas. In the tropical Pacific west of 160°E and in the eastern tropical Indian Ocean, the barrier-layer width changes by approximately 5 m in response to a 10-unit change in the Southern Oscillation index. It thickens during La Niñas as a result of the presence of abundant rainfall and thins during dry El Niños. Interannual variations of barrier-layer width in the equatorial Pacific are weak east of 160°E with an exception of the area surrounding the eastern edge of the warm pool. Here subduction of salty water contributes to locally stronger variations of barrier-layer width.

1. Introduction

The ocean mixed layer is a near-surface layer of fluid with quasi-uniform properties such as temperature, salinity, and density. The width of this mixed layer and its time rate of change both strongly influence the ocean's role in air–sea interaction. However, the width of the near-surface layer of quasi-uniform temperature (MLT) may differ from the width of the near-surface layer of quasi-uniform density (MLD). MLT may be thicker than MLD when positive salinity stratification forms a barrier layer (BL = MLT − MLD) isolating the shallower and deeper levels of the mixed layer as was originally found in the western equatorial Pacific (Lukas and Lindstrom 1991). Elsewhere MLT may be thinner than MLD when negative salinity stratification compensates for positive temperature stratification (or the reverse situation) to form a compensated layer (CL = MLD − MLT) (Stommel and Fedorov 1967; Weller and Plueddemann 1996). Changes in the seasonal width of BLs and CLs from one year to the next may cause corresponding changes in the role of the mixed layer in air–sea interaction by altering the effective depth of the mixed layer or the temperature of water at the mixed layer base (e.g., Ando and McPhaden 1997). Here we examine the global historical profile observations covering the period 1960–2007 for evidence of corresponding year-to-year changes in the BL and CL width distribution.

Four studies—Sprintall and Tomczak (1992), Tomczak and Godfrey (1994), de Boyer Montégut et al. (2007), and Mignot et al. (2007)—have provided an observational description of the seasonal cycle of BL and CL distribution over much of the global ocean. BLs are a persistent feature of the tropics as well as the high latitudes during winter. Spatial distribution of BLs in the

Corresponding author address: Semyon Grodsky, Department of Atmospheric and Oceanic Science, University of Maryland, College Park, College Park, MD 20742.
E-mail: senya@atmos.umd.edu

DOI: 10.1175/2009JCLI2974.1

tropics resembles spatial distribution of the surface freshwater flux. Here BLs occur in regions of high rainfall and river discharge such as the Arabian Sea and Bay of Bengal, where layers as thick as 20–60 m have been observed (Thadathil et al. 2008). Similarly, BLs occur in the western equatorial Pacific under the high precipitation regions of the intertropical convergence zone (ITCZ) and South Pacific convergence zone (Lukas and Lindstrom 1991; Ando and McPhaden 1997) and in the western tropical Atlantic (Pailler et al. 1999; Ffield 2007).

Impacts of the freshwater forcing on BLs are also evident at high latitudes. Here BLs occur where freshening in the near surface is produced by excess precipitation over evaporation, river discharge, or ice melting (de Boyer Montégut et al. 2007). In particular, in the Southern Ocean south of the Polar Front BLs occur as a result of near-surface freshening due to ice melting and weak thermal stratification (e.g., de Boyer Montégut et al. 2004). BLs produced by the surface freshening may be most evident in regions where upward Ekman pumping (w_{Ek}) acts against the effects of vertical mixing such as occurs in the North Pacific subpolar gyre (Kara et al. 2000). In addition to local air–sea interactions, the cross-gyre transport of salty and warm Kuroshio water from the subtropical gyre (which spreads in the subpolar gyre below the fresh mixed layer) contributes to the formation of a stable haline stratification and thus allows a cool mixed layer to exist over a warmer thermocline during winter–spring in the North Pacific subpolar gyre (Ueno and Yasuda 2000; Endoh et al. 2004).

At lower latitudes there is a remarkable regularity of BLs appearance equatorward of the subtropical salinity maxima (e.g., Sato et al. 2004). In the subtropical gyres the salinity is high because of permanent excess of evaporation over precipitation and the Ekman downwelling. Here BLs are present because of the subsurface salinity maximum produced by subduction and equatorward propagation of salty water. The subtropical North Pacific provides an example of this. In this region BLs are the result of subduction and southward propagation of salty North Pacific Subtropical Mode Water below fresher tropical surface water (Sprintall and Tomczak 1992).

Much less is known about subseasonal variations of BLs and CLs. In their examination of mooring time series Ando and McPhaden (1997) show that BLs do have interannual variability in the central and eastern equatorial Pacific and conclude that the major driver is precipitation variability associated with El Niño. At 0° 140°W, for example, the BL width increased from 10 to 40 m in response to the enhanced rains of the 1982/83 El Niño. Precipitation is particularly strong over the western Pacific warm pool. Intense atmospheric deep convection over the high SSTs of the warm pool produces heavy rainfall that promotes formation of thick salt-stratified BLs that, in turn, keep the warm pool SSTs high (Ando and McPhaden 1997). In addition to rainfall, ocean dynamics also contributes to formation of BLs in the western equatorial Pacific. At the seasonal time scales Mignot et al. (2007) suggest that changes in zonal advection in response to seasonally varying winds and wind-driven convergence are important in regulating BLs at the eastern edge of the western Pacific warm pool. Recent observations of Maes et al. (2006) indicate a close relationship between the longitude of the eastern edge of the warm pool, high SSTs, and the presence of barrier layers. During ENSO cycles the eastern edge of the warm pool shifts in the zonal direction that produces related interannual changes of BLs. In the west observational studies by Cronin and McPhaden (2002) and Maes et al. (2006) document the response of the mixed layer to intense westerly wind bursts, their fetch, and accompanying precipitation and show how these lead to both the formation and erosion of BLs.

CLs in contrast may result from excess evaporation over precipitation, such as occurs in the subtropical gyres, or by differential advection where it leads to cooler fresher surface water overlying warmer saltier subsurface water (Yeager and Large 2007; Laurian et al. 2009). De Boyer Montégut et al. (2004) summarize several additional possible mechanisms of CL formation, such as subduction-induced advection, Ekman transport, slantwise convection, and density adjustment. CLs are most prominent in the eastern subpolar North Atlantic and in the Southern Ocean (de Boyer Montégut et al. 2007). In the eastern North Atlantic a CL is formed by transport of the warm and salty North Atlantic Current above fresher colder subpolar water. Farther east the North Atlantic Current splits into a northern branch comprising the Norwegian and Irminger Currents and the southward Canary Current, all of which also develop CLs.

Climatological impacts of BLs and CLs have not been comprehensively understood yet. Although the ocean salinity does not have a direct impact on air–sea interactions or SST, the salinity stratification can feed back indirectly to the atmosphere through its influence on the upper-ocean density stratification (Ando and McPhaden 1997; Maes et al. 2006; Ffield 2007). In particular, Maes et al. (2006) suggest that the presence of a BL suppresses heat exchange between the mixed layer and the thermocline by reducing or cutting off entrainment cooling and trapping the heat and momentum fluxes in a shallow surface layer. Thus, a positive feedback between barrier-layer formation and warm SSTs is

possible. This positive feedback can ultimately lead to formation of SST hot spots (SST > 29.75°C) observed at the eastern edge of the Pacific warm pool (Waliser 1996). Foltz and McPhaden (2009) have found that erroneous BLs can bias SST simulations because of improper representation of heat exchange across the bottom of the mixed layer. Much less is known about potential feedbacks of CLs on SST and the atmosphere. Arguably, density compensation within CLs enhances heat exchanges across the bottom of the mixed layer and thus should provide a negative feedback on SST.

In this study we build on previous observational examinations of the seasonal cycle of BL and CL development to explore year-to-year variability. This study is made possible by the extensive 7.9 million hydrographic profile dataset contained in the *World Ocean Database 2005* (Boyer et al. 2006) supplemented by an additional 0.4 million profiles collected as part of the Argo observing program. We focus our attention primarily on the Northern Hemisphere because of its higher concentration of historical observations.

2. Data and methods

This study is based on the combined set of temperature and salinity vertical profiles archived in the *World Ocean Database 2005* (*WOD05*) for the period 1960–2004 and Argo floats from 1997 to 2007. Data quality control and processing are detailed in Carton et al. (2008), who used the *WOD05* profile inventory to explore subseasonal variability of global ocean mixed layer depth.

Mixed layer depth is defined here following Carton et al. (2008) [which in turn combines the approaches of Kara et al. (2000) and de Boyer Montégut et al. (2004)] as the depth at which the change in temperature or density from its value at the reference depth of 10 m exceeds a specified value (for temperature: $|\delta T| = 0.2$°C). This reference depth is sufficiently deep to avoid aliasing by the diurnal signal but shallow enough to give a reasonable approximation of monthly SST. Because the definition of mixed layer depth is based on the 10-m reference depth, our examination misses features like shallow freshwater lenses (just after intense rainfalls) and other transient processes in the very upper-10-m column. The value of $|\delta T| = 0.2$°C is chosen following de Boyer Montégut et al. (2004) as a compromise between the need to account for the accuracy of mixed layer depth retrievals and the need to avoid sensitivity of the results to measurement error. The absolute temperature difference instead of the negative temperature difference is used following Kara et al. (2000) in order to accommodate for temperature inversions that are widespread at high latitudes.[1] The specified change in density used to define the density-based mixed layer depth follows the variable density criterion (e.g., Sprintall and Tomczak 1992) to be locally compatible with the specified temperature value [i.e., $\delta\rho = (\partial\rho/\partial T) \times 0.2$°C]. In this study the width (or thickness) of either a barrier layer or compensated layer is defined as a difference of isothermal mixed layer depth and isopycnal mixed layer depth, MLT − MLD. The difference MLT − MLD is referred to as BL/CL width in this paper. As a result of these definitions a positive MLT − MLD difference (BL/CL width > 0) indicates the presence of a BL, while a negative MLT − MLD difference (BL/CL width < 0) indicates the presence of a CL. We compute BL/CL width for each profile. These data are then passed through a subjective quality control to eliminate outliers and averaged into 2° × 2° × 1-month grid without any attempt to fill in empty bins.

The total number of binned MLT observations on a 2° × 2° monthly grid during 1960–2007 is 1 021 580. Many of these observations are obtained from temperature-only profiles measured by either expendable or mechanical bathythermographs; there are only 364 228 (or ~35%) binned MLD observations. As expected, the spatial coverage of both MLT and MLD is weighted toward the Northern Hemisphere. North of 10°S there are 271 157 MLD and 788 204 binned MLT observations (~75% of the global total). In this study we use only those vertical casts where both T and S are available; consequently, numbers of MLT and MLD observations in this data subset are equal. This study focuses on the cold season variability in each hemisphere. Because the peak of mixed layer deepening lags the midmonth of calendar winter by around one month, we choose January–March (JFM) and July–September (JAS) averages to characterize conditions during northern and southern winter, respectively.

We explore the role that surface forcing plays in regulating mixed layer properties through comparison of the BL/CL distribution to fluxes from the National Centers for Environmental Prediction–National Center for Atmospheric Research (NCEP–NCAR) reanalysis of Kalnay et al. (1996). Satellite Quick Scatterometer (QuikSCAT) winds (see Liu 2002), which begin in mid-1999, are used to characterize the finer-scale spatial patterns of w_{Ek}. To better characterize precipitation in the tropics, we also examine the Climate Prediction Center

[1] For an example for the vertical profile shown in Fig. 1b of de Boyer Montégut et al. (2007), our criterion places the MLT at the top of the warm temperature inversion layer while the de Boyer Montégut et al. (2007) criterion includes the entire subsurface warm layer into the isothermal mixed layer.

TABLE 1. Bulk Turner angle and idealized vertical profiles of temperature and salinity corresponding to CL and BL; $T_z = \partial T/\partial z < 0$ implies stable stratification (z-axis is downward), and H_0 is isothermal or isohaline layer depth (whichever is shallower).

CL	BL				CL
Bulk Turner angle					
-90° $\tan^{-1}(-3)$	$\tan^{-1}(-3)$ - 45°	-45°	-45° 45°	45°	45° 90°
Vertical T-(solid) and S-(dashed) profiles					
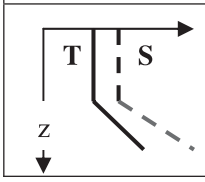	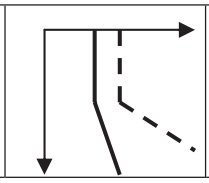	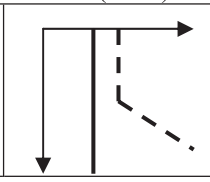	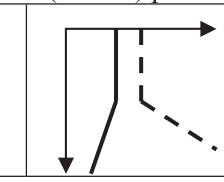	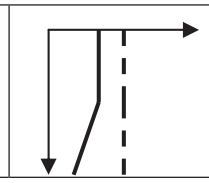	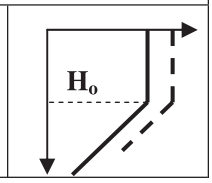

Merged Analysis of Precipitation (CMAP) of Xie and Arkin (1997), which covers the period 1979–present.

To quantify the relative impact of temperature and salinity stratification within BLs and CLs we use a bulk Turner angle, defined following Ruddick (1983) as $\mathrm{Tu}_b = \tan^{-1}[(\alpha\Delta T - \beta\Delta S)/(\alpha\Delta T + \beta\Delta S)]$, where $\alpha = \rho^{-1}\partial\rho/\partial T$ (negative) and $\beta = \rho^{-1}\partial\rho/\partial S$ (positive) are the expansion coefficients due to temperature T and salinity S. For negative α our definition of Tu_b is consistent with Yeager and Large (2007). In this study the changes in temperature and salinity ΔT and ΔS are computed between the top, $z_t = \min(\mathrm{MLT}, \mathrm{MLD})$, and the bottom, $z_b = \max(\mathrm{MLT}, \mathrm{MLD})$, of either a BL or CL based on analysis of individual vertical profiles. The bulk Turner angle is then evaluated from spatially binned values of ΔT and ΔS.

There are correspondences between the BL/CL width and the Turner angle. They are illustrated in Table 1 using idealized vertical T and S profiles that include a perfectly homogeneous mixed layer of depth H_0 (isothermal or isopycnal whichever is shallower) with a thermocline and halocline beneath where temperature and salinity vary linearly with depth (z). If the top of thermocline is above the top of halocline, the vertical stratification just below $z = H_0$ is similar to the freshwater case ($\partial S/\partial z = S_z = 0$), so that BL = 0 and $\mathrm{Tu}_b = 45^\circ$. In contrast, if the top of halocline is above the top of thermocline, the vertical thermal stratification just below $z = H_0$ is absent ($\partial T/\partial z = T_z = 0$), and the BL width could vary significantly while $\mathrm{Tu}_b = -45^\circ$. If the top of halocline is at the same depth ($z = H_0$) as the top of thermocline, the mixed layer depth based on temperature and density criteria is expressed via corresponding difference criteria ($|\delta T| = 0.2^\circ\mathrm{C}$, $\delta\rho = -\alpha|\delta T|$) and vertical gradients, $\mathrm{MLT} = H_0 + |\delta T|/|T_z|$, and $\mathrm{MLD} = H_0 + \delta\rho/\rho_z$. Switching between the CL and BL regimes occurs when $\mathrm{BL} = \mathrm{MLT} - \mathrm{MLD} = |\delta T|/|T_z| - \delta\rho/\rho_z$ is zero. Noting that $\rho_z = \alpha T_z + \beta S_z$, two solutions of BL = 0 exist depending on the sign of T_z. If thermal stratification is stable ($T_z < 0$), BL = 0 if salinity is homogeneous in the vertical ($S_z = 0$) and $\mathrm{Tu}_b = 45^\circ$. If thermal stratification is unstable ($T_z > 0$), BL = 0 if $2\alpha T_z + \beta S_z = 0$ and $\mathrm{Tu}_b = \tan^{-1}(-3) \approx -72^\circ$.

As seen from the above analysis, the BL width is not a unique function of the Turner angle. For a given δT it also depends on $\delta\rho$ (which is a function of T and S) and on the vertical gradients. In addition, the mixed layer is only approximately homogenous, a fact that contributes to scatter of mixed layer depth (and BL/CL width) estimates especially in situations with weak stratification. Nevertheless, analysis of observed vertical profiles shows a distinct correspondence between values of ΔT, ΔS, and Tu_b and the presence of BLs and CLs (Fig. 1). Angles $|\mathrm{Tu}_b| < 45^\circ$ correspond to BLs stabilized by both temperature and salinity ($\Delta T > 0$, $\Delta S < 0$). A BL stabilized by salinity but homogeneous in T corresponds to $\mathrm{Tu}_b = -45^\circ$, while $\mathrm{Tu}_b = 45^\circ$ corresponds to pure thermal stratification. Angles greater than 45° correspond to the most frequently occurring CLs where positive temperature stratification compensates for negative salinity stratification (the mixed layer is saltier than the thermocline). Less frequently occurring CLs below cool and fresh mixed layers ($-90^\circ < \mathrm{Tu}_b < -72^\circ$) are observed at high latitudes. The transition point of -72° is associated with the density ratio $R_\rho = -\alpha\Delta T/\beta\Delta S = 0.5$ or $\mathrm{Tu}_b = \tan^{-1}(-3) \approx -72^\circ$. For the majority of observed vertical profiles the bulk Turner angle varies between -45° and 90°. In this range of Tu_b the BL/CL width varies monotonically (to within the scatter of data) as a function of Tu_b (Fig. 1). Thus, the bulk Turner angle in this range provides an alternative way of displaying BL/CL distribution.

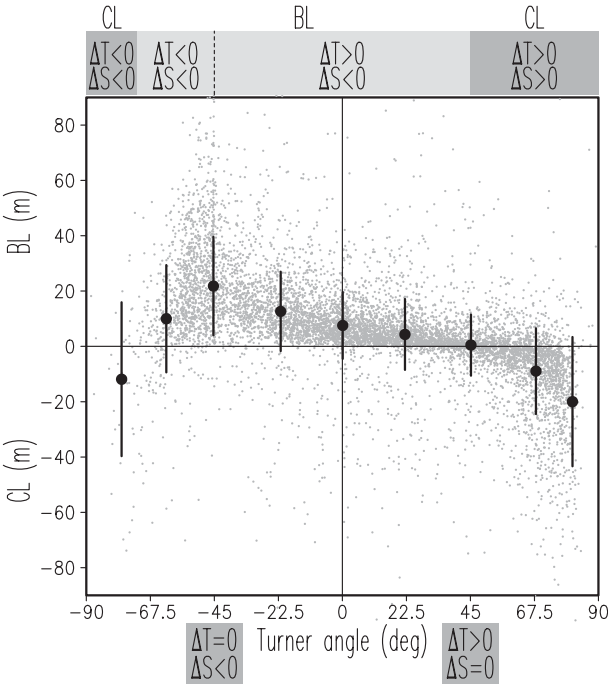

FIG. 1. Observed climatological winter–spring BL/CL width vs bulk Turner angle evaluated using temperature (ΔT) and salinity (ΔS) difference between the top and bottom of a barrier or compensated layer. Vertical bars show the mean and the standard deviation for consecutive 22.5° intervals. Gray dots show January–March data from the Northern Hemisphere and July–September data from the Southern Hemisphere. The Turner angle range of −72° to 45° corresponds to barrier layer. The compensated layer occurs outside this interval.

3. Results

a. Time mean and seasonal patterns

Global seasonal patterns of BL and CL display many features revealed by previous analyses (de Boyer Montégut et al. 2007). Throughout the year there are persistent BLs in the tropics in areas of high precipitation (Figs. 2a,b) where our estimates of BL width are similar to previous analysis. In particular, BLs are thick under the intertropical convergence zone and the South Pacific convergence zone. BLs are generally thickest on the western side of the tropical Pacific and Atlantic Oceans, reflecting higher levels of rain as well as (in the case of the Atlantic) Amazon River discharge. In both the western tropical Pacific and Atlantic Oceans salt advection contributes to the seasonal variation of salinity and BLs (Foltz et al. 2004; Mignot et al. 2007). In contrast to the tropical Pacific and Atlantic (where BLs are thickest in the west) BLs are thickest on the eastern side of the tropical Indian Ocean because of the presence of the Java and Sumatra high precipitation area and freshwater transport from the Bay of Bengal (Qu and Meyers 2005). Rainfall in the southern intertropical convergence zone in the South Atlantic (Grodsky and Carton 2003) may contribute to freshening of the mixed layer along 10°S during austral winter. In midlatitudes, BL/CLs occur in each hemisphere mainly during local winter and early spring. In boreal winter BLs exceeding 60 m are observed in the North Pacific subpolar gyre (Fig. 2a). Similarly thick BLs occur in the Atlantic Ocean north of the Gulf Stream. In both locations the BLs appear coincident with a seasonal cooling of SST, weakening of thermal stratification, and deepening of MLT. In the North Pacific and the Labrador Sea our estimates of BL width are smaller than BL width by de Boyer Montégut et al. (2007). This difference is due to the difference in the definition of temperature-based mixed layer depth. As it is noted above, the de Boyer Montégut et al. (2007) MLT estimates are generally deeper in areas of subsurface temperature inversions because of inclusion of the entire depth range of temperature inversion into the mixed layer.

Sea surface salinity (SSS) increases drastically, moving from the cold sector to the warm sector across the Gulf Stream Front leading to a switch from the BL regime north of the front to a CL regime south of the front (Fig. 2a). Thick CLs (thicker than 30 m) are also observed along the Gulf Stream because of cross-frontal transport of low salinity water. And even thicker CLs (thicker than 60 m) are observed farther northeast along the path of the North Atlantic Current where its warm, salty water overlies cooler, fresher water.[2] Interestingly, despite the presence of warm and salty western boundary currents in both the Atlantic and Pacific Oceans, the winter CLs are much less pronounced in the North Pacific than the North Atlantic. An explanation for this basin-to-basin difference likely lies in the higher surface salinity of the Atlantic (Fig. 2a) and consequently larger values of ΔS (Fig. 3a).

CLs are evident in the southern subtropical gyres of the Pacific and Atlantic Oceans as well as the south Indian and southwest Pacific Oceans (Fig. 2b) south of the 30°S SSS maximum. The presence of CLs in these regions reflects the northward advection of cold and freshwater, which subducts (because of the downward Ekman pumping) under the water of the SSS maximum (Sprintall and Tomczak 1993; Laurian et al. 2009). Note the correspondence between CL in Fig. 2b and ΔS in Fig. 3b. A similar subduction mechanism may explain BL formation in subtropical gyres (e.g., Sato et al. 2004).

[2] CLs in the North Atlantic and Southern Ocean are not displayed in Fig. 3 of de Boyer Montégut et al. (2007) because these CLs have a width that is less than 10% of MLD according to their analysis.

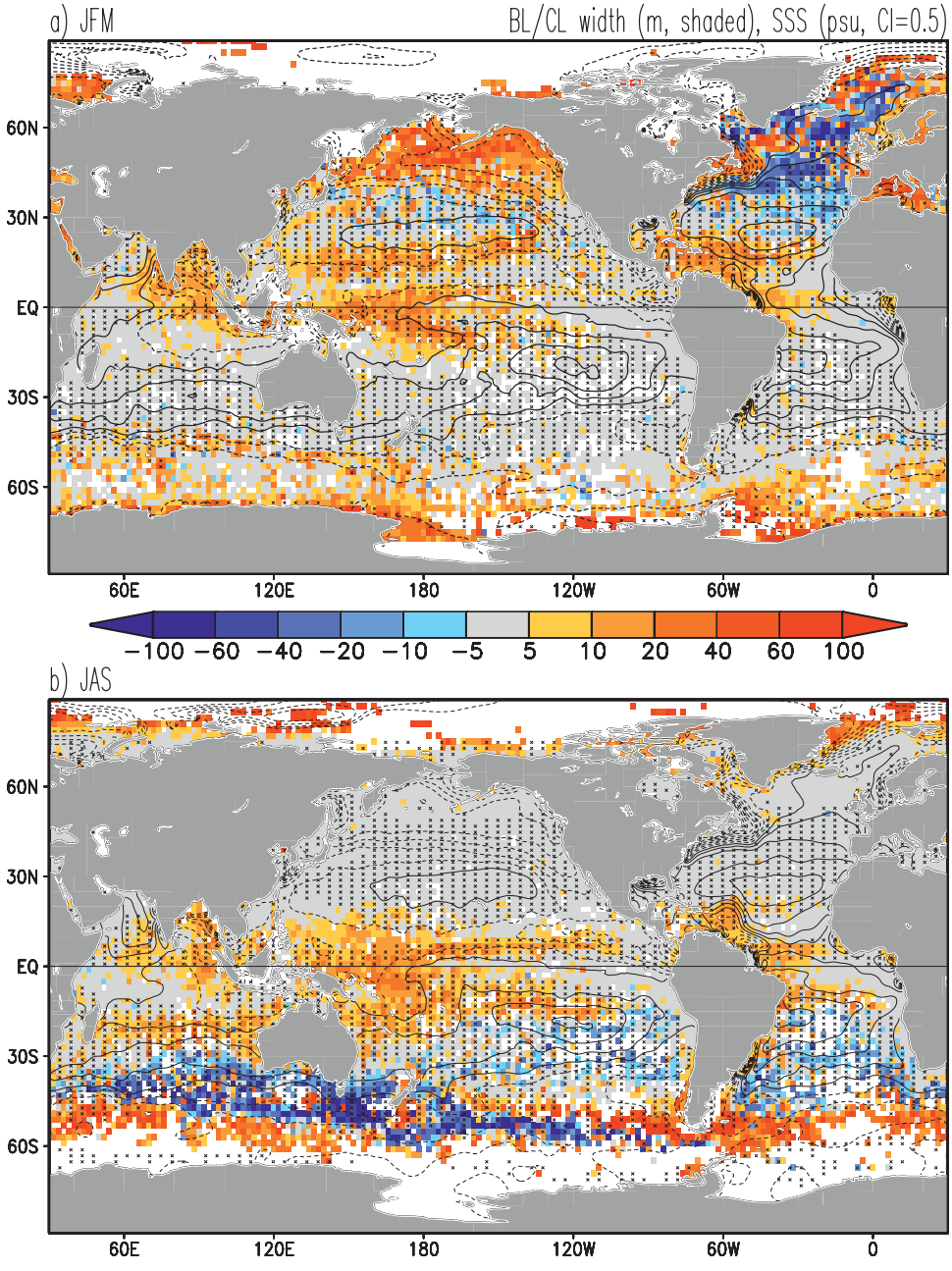

FIG. 2. Observed climatological (a) January–March and (b) July–September barrier-layer width (positive) and compensated-layer width (negative): climatological SSS (Boyer et al. 2006; contours), SSS ≥ 35 psu (solid), and SSS < 35 psu (dashed). Areas of downward Ekman pumping are crosshatched. Ekman pumping is evaluated from the QuikSCAT scatterometer winds of Liu (2002).

In particular, in the southern Indian Ocean north of 30°S, BLs form as a result of subduction of salty water from the region of the SSS maximum and the northward propagation of this salty water under relatively fresh surface water (Fig. 2b).

The subduction mechanism suggests the BL presence equatorward of the subtropical SSS maximum (where mixed layer tops saltier water below) and the CL presence poleward of the subtropical SSS maximum (where mixed layer is saltier than thermocline). This is evident in a dipole-like meridional pattern of CL and BL in the southern Indian Ocean and adjusted part of the Southern Ocean encompassing the area of SSS maximum along 30°S. Similar meridional dipole-like patterns with

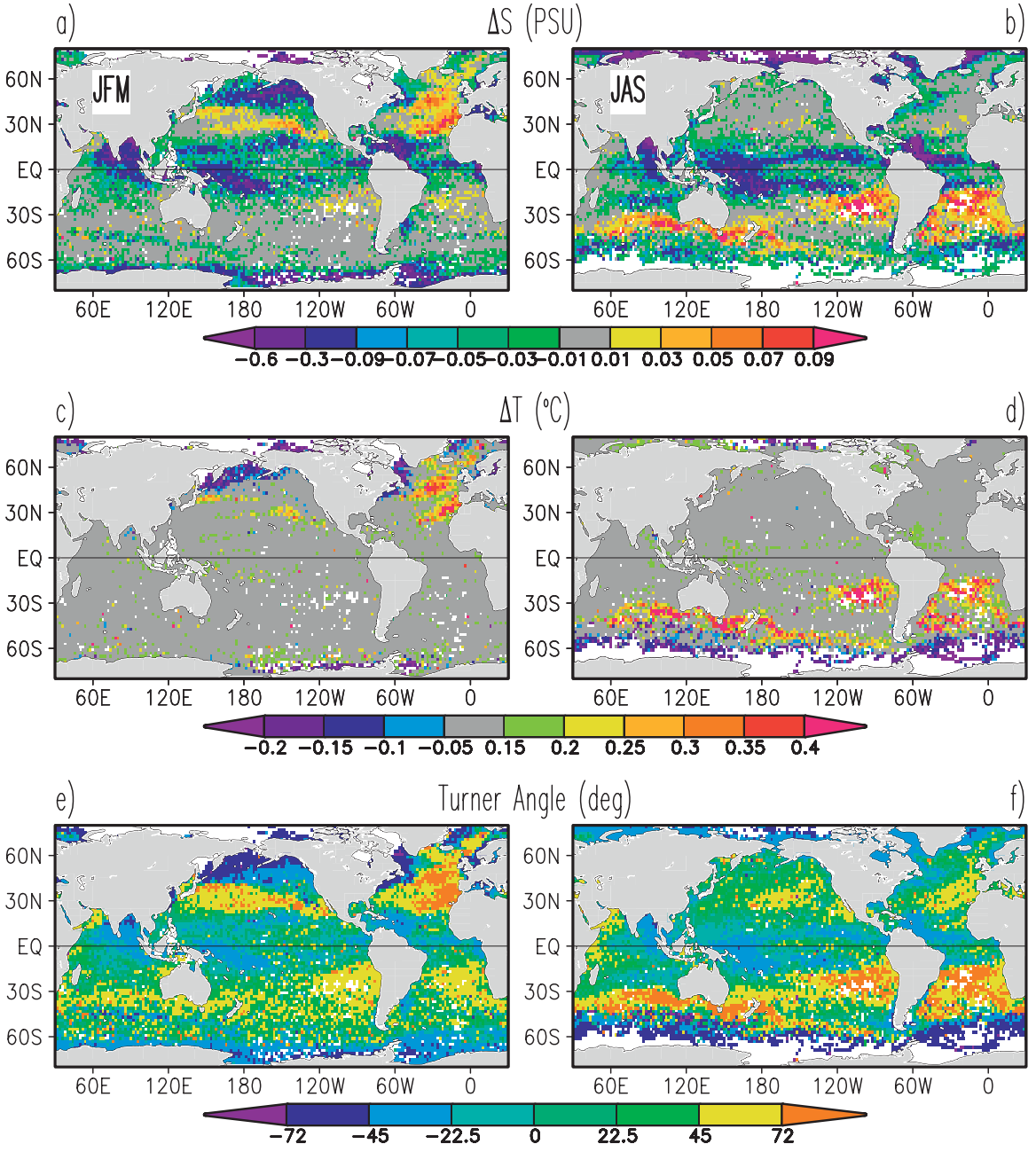

FIG. 3. Observed (a),(b) salinity (ΔS) and (c),(d) temperature (ΔT) difference between the top z_t = min(MLT, MLD) and bottom z_b = max(MLT, MLD) of BL/CL; (e),(f) bulk Turner angle calculated from ΔS and ΔT between the same two depths. (a),(c),(e) JFM values; (b),(d),(f) JAS values. Turner angles in the range from −72° to 45° correspond to barrier layers, while compensated layers occur outside this range.

CLs to the south and BLs to the north of local subtropical SSS maxima are seen during austral winter in the South Pacific and the South Atlantic in the regions of downward w_{Ek} (Fig. 2b).

This also appears to hold in the subtropics of the Northern Hemisphere (Fig. 2a). In the North Atlantic CLs are observed north of the subtropical SSS maximum (as expected from the subduction mechanism). But in boreal winter the maximum width CLs in the North Atlantic are observed well north of the downward w_{Ek} regions (Fig. 2a). Here CLs extend along the Gulf Stream path and its northern extensions. This, in turn, suggests that in the North Atlantic the horizontal transport of warm salt waters by the western boundary current (rather

than the subduction mechanism) contributes to regional CL formation.

Both BLs and CLs accompanying the subtropical maximum of SSS are strongly seasonal (Fig. 2) in spite of the permanent presence of subtropical SSS maximum and the Ekman downwelling maintained by trade winds. Mignot et al. (2007) have suggested that these permanent factors form background haline stratification while the seasonal variability of BLs is explained by the seasonal deepening of the local MLT during the cold season due to intense wind stirring and negative buoyancy forcing and the presence of a shallow capping halocline. In fact, equatorward of the SSS maximum the subsurface salinity is relatively high because of the presence of salty Subtropical Underwater subducted in the region of the SSS maximum, while the surface salinity is relatively low because of the poleward wind-driven advection of fresh equatorial waters (Foltz et al. 2004). In the CL sector the same seasonal deepening of the mixed layer explains the seasonal widening of CLs. Here the injection of saltier mixed layer water into a fresher thermocline (the ''spice injection'' mechanism of Yeager and Large 2007) results in stronger density compensation and the widening of CLs during local winter (Fig. 2).

Spatial patterns of BL/CL width (Fig. 2) are in close correspondence with the spatial patterns of the vertical changes of salinity ΔS (Figs. 3a,b). As expected, the BLs are distinguished by a stable salinity stratification $\Delta S < 0$, where salinity increases downward below the mixed layer. In contrast, CLs have unstable salinity stratification $\Delta S > 0$. As discussed above, regions of fresh mixed layer trace major areas of precipitation (like the intertropical convergence zone) and river runoff (the Bay of Bengal). A different type of BL is observed on the equatorward flanks of the subtropical SSS maxima. In these areas the ocean accumulates salt because of an excess of evaporation over precipitation. As discussed in the previous paragraph, here the equatorward propagation of subducted water produces meridional dipole-like BL/CL and ΔS structures that are most pronounced in the Southern Hemisphere during austral winter (Figs. 2b, 3b).

The spatial patterns of the bulk Turner angle (Figs. 3e,f) indicate that the majority of CL cases are associated with warm, salty mixed layer water overlying colder, fresher water beneath (thus $\mathrm{Tu}_b > 45°$). Much rarer CLs can also be formed when cold freshwater overlays warmer, saltier water ($\mathrm{Tu}_b < -72°$). This latter type of density compensation is observed only in limited regions of the Labrador Sea during northern winter and near Antarctica during austral winter. The most commonly observed CLs associated with warm and saltier mixed layers ($\mathrm{Tu}_b > 45°$) increase in width during the cold season. This seasonal widening of CL width is attributed by Yeager and Large (2007) to the seasonal increase in Tu_b that is produced by the spice injection and results in stronger density compensation, and thus thicker CLs. The similarity of Figs. 3e,f to Fig. 7 of Yeager and Large (2007) where Tu_b is computed in the upper 200-m column indicates that during the cold season the vertical changes of temperature and salinity within the BL/CL depth range have the same sign and roughly the same magnitude as the vertical changes across the upper 200-m water column. But, in the tropical Pacific and Atlantic (where the mixed layer is rather shallow), the Yeager and Large (2007) analysis shows significant areas of $\mathrm{Tu}_b > 45°$. In contrast, our analysis in Fig. 3 indicates that CLs do not occur in these tropical areas. In these tropical areas $\mathrm{Tu}_b > 45°$ in the Yeager and Large (2007) analysis reflects density compensation due to stable thermal stratification and unstable haline stratification below the Equatorial Undercurrent core where both T and S decrease downward.

b. Subseasonal variability

Interannual and longer (subseasonal) variability of BL/CL width is similar in amplitude to seasonal variability (cf. Fig. 4 and Fig. 2). In the subtropics and midlatitudes this variability occurs in winter–spring of each hemisphere when BL/CLs are present. During the rest of the year when subtropical and midlatitude mixed layers warm and shoal the BL/CLs collapse, so BL/CL width variability is weak. In the tropics BL/CLs are always present and so is their variability. In particular, the variability of BLs in the western tropical Pacific is ~50% (or more) of the time mean BL width, which is 10–40 m in this region (Figs. 2 and 4). This BL variability reflects interannual variations of rainfall and currents due to ENSO (Ando and McPhaden 1997). In the western equatorial Atlantic as well the BLs are quasi-permanent because of Amazonian discharge and ITCZ rainfall (Pailler et al. 1999; Foltz et al. 2004). Interannual variability of BLs in this region is comparable in width to the time mean BL width, which is 5–20 m. This interannual variability is produced by interannual variation of river discharge as well as by anomalous meridional shifts of the Atlantic ITCZ. Time-mean BLs vanish and their subseasonal variability is weak in the eastern tropical Atlantic and Pacific and along the eastern subtropical coasts of the Atlantic and Pacific (Fig. 4), where the mixed layer shoals because of equatorial and coastal upwellings. The zonal distribution of BL width variability is reversed in the tropical Indian Ocean where BLs are thickest, and their variability is stronger in the east because of strong rainfall over the Maritime Continent

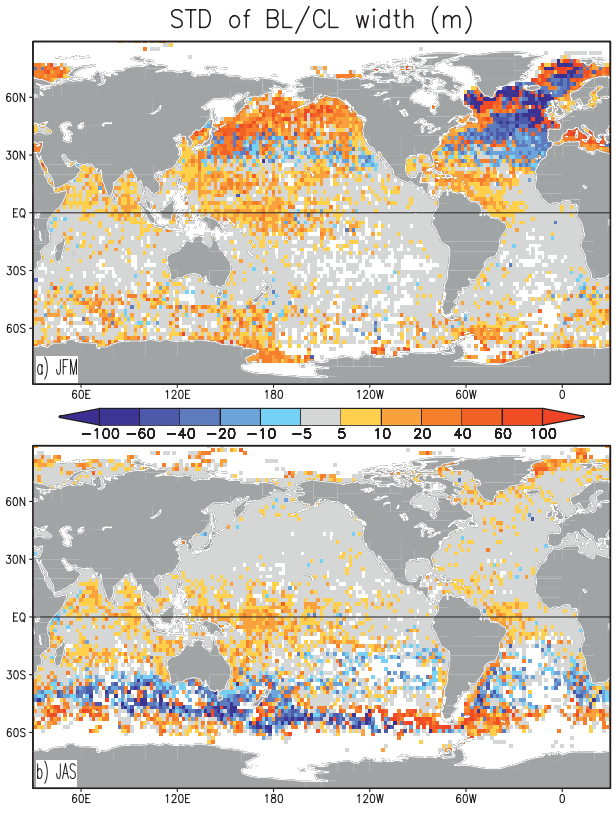

FIG. 4. Standard deviation (std dev) of observed (a) JFM and (b) JAS averaged BL/CL width. To contrast variability of BL and CL width, std dev is multiplied by the sign of corresponding 3-month average climatological BL/CL width; so the std dev of BL and CL width is positive and negative, respectively. All values are computed from the 1960–2007 data.

and surrounding areas as well as freshwater transport from the Bay of Bengal.

Subseasonal variability is stronger at higher latitudes, reflecting weaker temperature stratification there. Weaker temperature stratification implies a stronger relative impact of freshwater fluxes and other factors on density stratification. The highest variability of BL/CL width (of up to 100 m) occurs in winter in the North Atlantic along the routes of northward propagation of warm and salty Gulf Stream water. In these regions the vertical temperature and salinity stratification is similar to that in the subtropical gyres where CLs are formed as a result of the presence of a warmer and saltier mixed layer above a fresher thermocline. As warm and salty Gulf Stream water propagates northward, the temperature stratification weakens (because of the surface cooling), so CLs widen.

Spatial patterns of CLs are different in the North Pacific in comparison with the North Atlantic. In contrast to the North Atlantic, the near-surface layer is relatively fresh in the North Pacific in response to abundant local rainfall. This surface freshwater forcing produces stable haline stratification. In addition to that the haline stratification is affected by exchanges across the Kuroshio–Oyashio Extension front. These exchanges result in the expansion of Kuroshio waters into the subpolar gyre where they form a warm and salty subsurface maximum (Endoh et al. 2004). This stable halocline is further maintained by the surface freshwater flux and the upward Ekman pumping. In winter when the MLT deepens in response to the surface cooling, this stable halocline produces 20–60-m-wide BLs (Fig. 2a) with subseasonal variation of similar magnitude (Fig. 4a).

Time correlations of anomalous BL/CL width with other mixed layer parameters suggest the mechanisms that govern the subseasonal variability of BL/CL. In Fig. 5 we focus on the northern winter (JFM) when BL/CL width increases in the Northern Hemisphere. These data allow only qualitative examination because of short time series. During JFM, only ~50 000 gridded observations are available globally; that translates into an average of five observations at each grid point, so only large-scale correlation patterns matter. Over much of the global ocean BL/CL width is negatively correlated with the bulk Turner angle (Fig. 5a). Most BL cases are associated with fresh mixed layers and stable thermal stratification ($-45° < \mathrm{Tu}_b < 45°$) whereas most CL cases are associated with salty mixed layers ($45° < \mathrm{Tu}_b < 90°$) (Fig. 3). In this combined range $-45° < \mathrm{Tu}_b < 90°$ the BL/CL width decreases with increasing Tu_b (Fig. 1). In some northern areas—including the subpolar Pacific, the cold sector of the Gulf Stream, and the Norwegian Sea—BL width is positively correlated with Tu_b. All these areas are distinguished by the presence of temperature inversions bottoming fresh BLs (Figs. 3a,c). These vertical stratifications correspond to $-72° < \mathrm{Tu}_b < -45°$ where the BL width increases with Tu_b (Fig. 1). BL width reaches maximum at $\mathrm{Tu}_b = -45°$, which corresponds to shallow fresh BL inside a deeper homogeneous temperature layer.

Negative correlations between BL/CL width and MLD are similarly widespread (Fig. 5b). For BLs this negative correlation means that the shallower the fresh density-based mixed layer is, the wider the depth range separating the bottom of the MLT and MLD. For CLs that are associated with salty mixed layers, deepening of the density-based mixed layer suggests salt injection into the thermocline leading to stronger density compensation and wider CLs (Yeager and Large 2007). In contrast to mostly negative correlation with MLD, BL/CL width tends to be positively (negatively) correlated with depth of MLT in barrier-layer (compensated layer) regions, respectively (Fig. 5c). The positive correlation in BL regions is better seen and may be explained using the

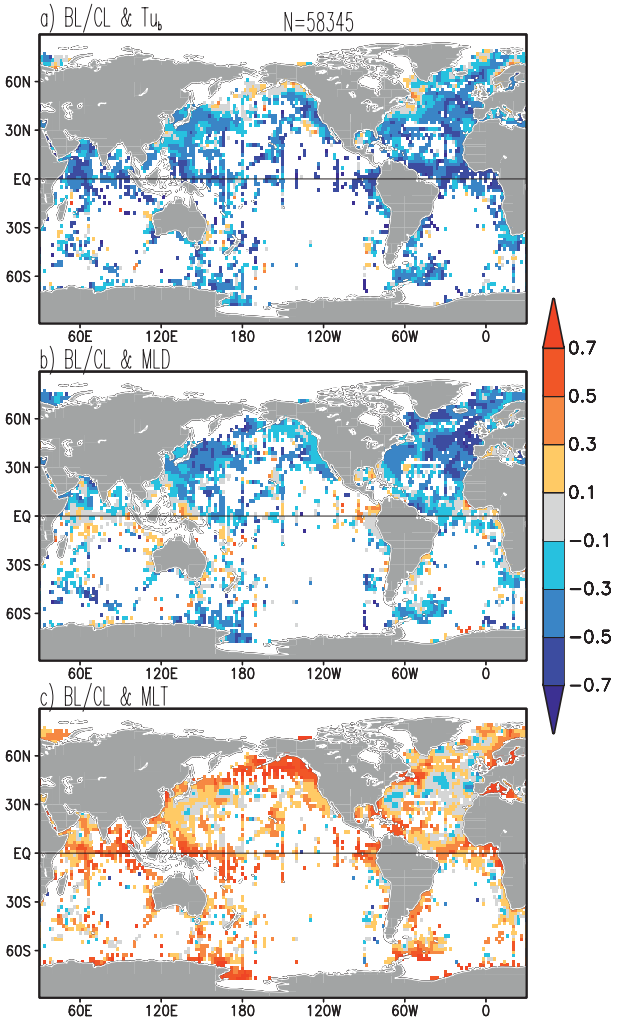

FIG. 5. Time correlation of January–March average (a) BL/CL width and bulk Turner angle, (b) BL/CL and density-based mixed layer depth, and (c) BL/CL and temperature based mixed layer depth. Here N is the total number of JFM average binned observations during 1960–2007. Correlations are shown only at grid points where at least 6 observations are available. Time correlation at every grid point is not significant; only large-scale patterns matter.

same arguments as those employed by Mignot et al. (2007) to explain the seasonal variability of BLs. A variety of factors (surface freshwater fluxes, freshwater advection, etc.) produce shallow haline stratification. Year-to-year changes in the surface forcing affect the seasonal deepening of the MLT during the cold season. In the presence of a shallow capping halocline, these interannual variations of MLT (which define the base of the BL) explain variations of BL width.

We next consider BL/CL width separated by season and roughly 15-year averaging periods (Fig. 6). In contrast to significant variability of anomalous BL/CL width on interannual and longer periods (Fig. 4), the decadal means are similar during the three averaging periods shown in Fig. 6. This suggests that much of the BL/CL width variability occurs at interannual periods except in the North Pacific where long-term changes are also detectable. During the first period of 1960–75, thick BLs are evident during local winter in the North Pacific, western tropical Pacific and Atlantic, northern Indian Ocean, and Southern Ocean (the latter being evident even in austral summer). CLs during this early period appear primarily in the eastern North Atlantic. Little can be said about the existence of BLs in the Southern Ocean in austral winter because of the lack of data during this period. By the latest period, 1991–2007, several changes are evident. CLs have appeared in the subtropical North Pacific during winter, replacing BLs. Elsewhere in the North Pacific the width of the BLs has shrunk. Vertically wide CLs are also evident on the northern side of the Circumpolar Current during austral winter (in fact these may have existed earlier but simply had not been observed). In contrast to the North Pacific the North Atlantic does not exhibit similar long-term changes (or these changes are not detectable with our dataset[3]) even though the winter–spring meteorology of this region does exhibit decadal variations (Hurrell 1995). The last period averages (1991–2007) are computed twice: including the latest Argo data (Figs. 6c,g) and based on the original *WOD05* profile inventory (Figs. 6d,h), which does not include massive Argo float deployments of recent years. The two averages look similar and confirm the presence of long-term changes of BL/CL width in the North Pacific. We next examine monthly time series of BL/CL width in the North Pacific focusing on two adjacent regions: 1) BLs in the subpolar North Pacific (NP/BL box) and 2) CLs in the subtropical North Pacific (NP/CL box) outlined in Fig. 6.

c. *North Pacific*

The monthly time series of the northern subpolar North Pacific BL region and the subtropical CL region both show long-term changes toward thinner BLs and thicker CLs interrupted by occasional interannual reversals (Figs. 7a,b). Indeed, the subtropical CL region actually supported a 10–20-m-thick BL prior to 1980s. One direct cause of this change from BL to CL is the

[3] Our data show interannual thickening of CLs in the North Atlantic in response to interannual strengthening of the North Atlantic Oscillation (NAO) during the Argo period (1997–2007), but the long-term response of CLs to the secular strengthening of the NAO during the second half of the twentieth century does not manifest in our dataset.

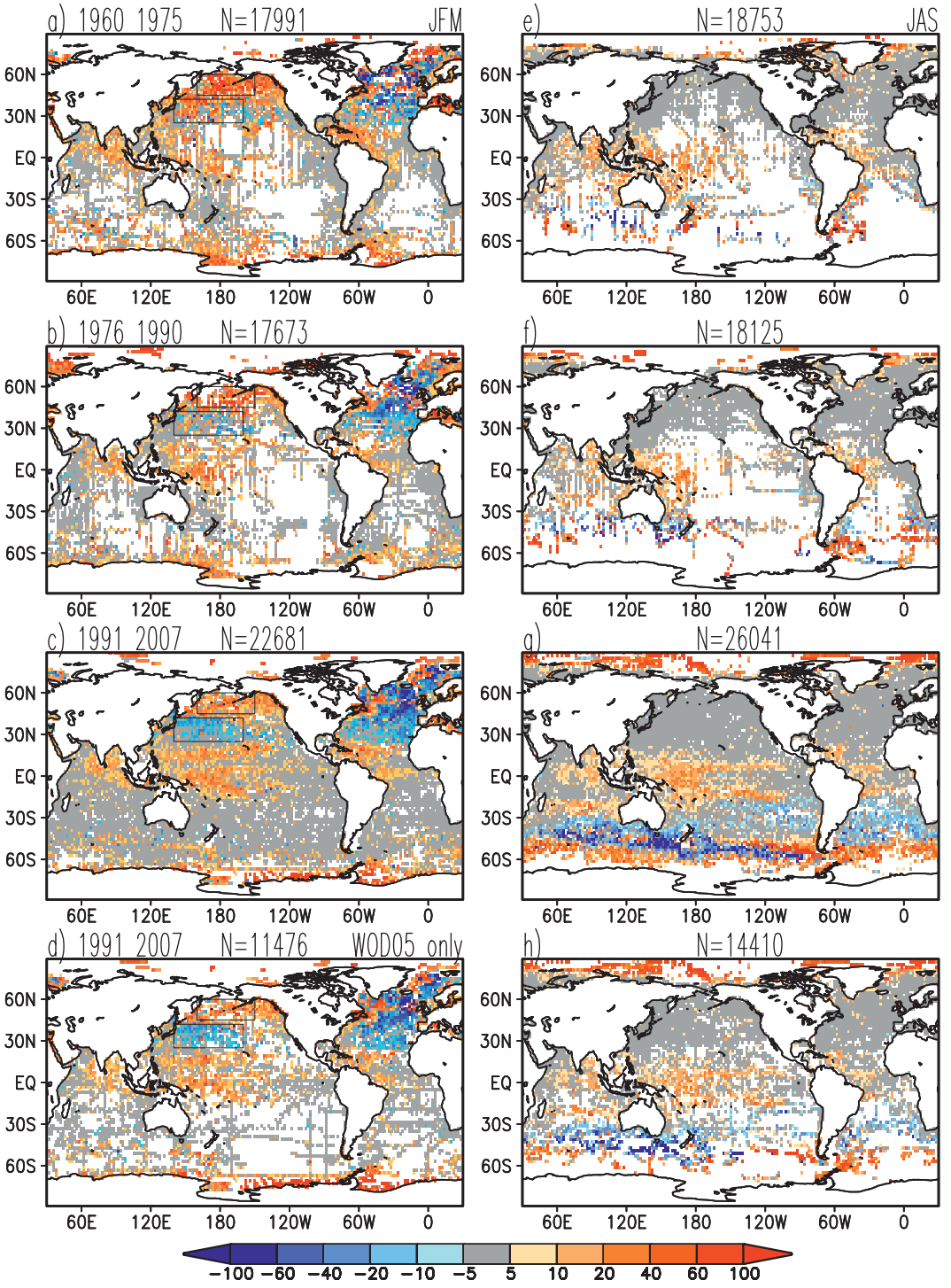

FIG. 6. Quasi-decadal average barrier-layer (positive) and compensated-layer (negative) width in (left) northern winter and (right) austral winter. Units are meters. Rectangles show locations of the North Pacific barrier-layer box (NP/BL; 45°–60°N, 160°E–150°W) and the North Pacific compensated-layer box (NP/CL; 25°–42°N, 140°E–160°W). (bottom row) The 1991–2007 averages based on the *WOD05* data, which do not include most of recent Argo data. Here N is the number of 3-month average observations accumulated during each 15-year period over the global ocean. There are a total of 11 000 ocean grid points on a $2° \times 2°$ grid.

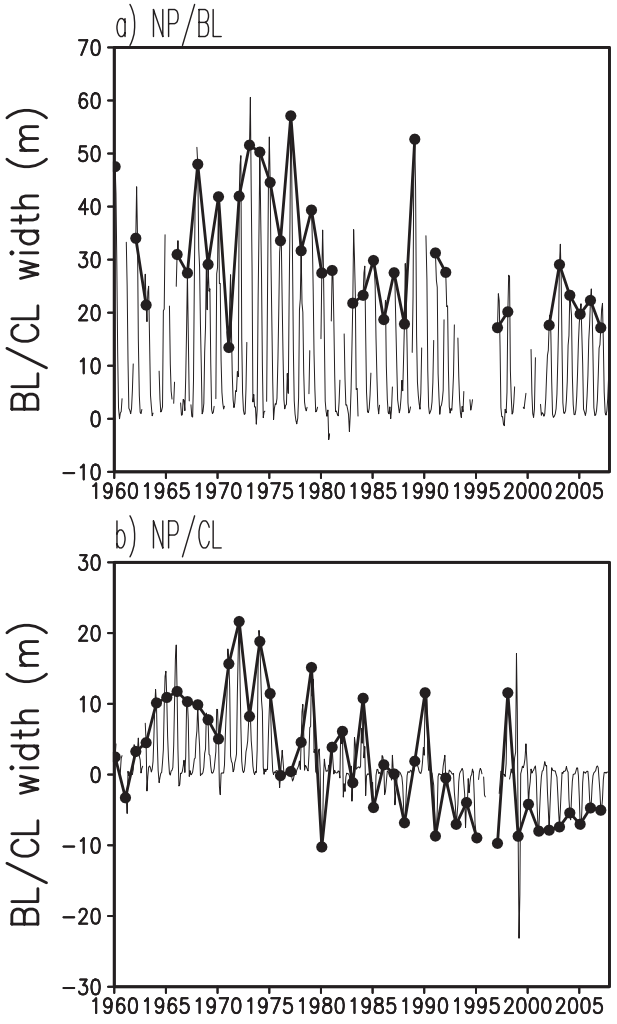

FIG. 7. Box-averaged BL/CL width in the (a) North Pacific barrier-layer region and (b) North Pacific compensated-layer region. Thin lines are 3-month running mean; bold lines are January–March averages. Data are shown if at least 10 measurements are available for box averaging. See Fig. 6 for box locations.

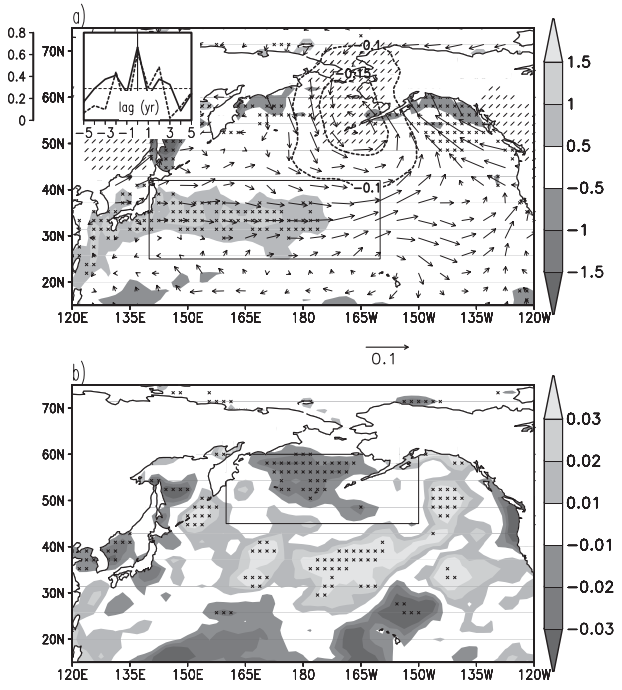

FIG. 8. Linear time regression of observed 1960–2007 anomalous JFM BL/CL width in the North Pacific compensated-layer box on anomalous (a) latent heat flux [W m^{-2} $(m)^{-1}$, shading], 10-m winds [m s^{-1} $(m)^{-1}$, arrows], and mean sea level pressure (hPa m^{-1}, contours); (b) surface precipitation rate (mm h^{-1} m^{-1}) elsewhere. BL/CL width time series is *inverted*, so that regressions correspond to widening of CLs and shrinking of BLs. Areas where time correlation with latent heat flux and precipitation is significant at the 95% level are X-hatched while similar areas for air pressure are /-hatched. Inlay shows lagged correlation of anomalous inverted BL/CL width and MLD averaged over (solid) the NP/CL box and (dashed) the NP/BL box. The two box locations are shown in (a) and (b), respectively. Dashed line is the 95% confidence level of zero correlation. Positive correlation at zero lag implies that CL thickens and BL thins when the mixed layer deepens. Atmospheric parameters are provided by the NCEP–NCAR reanalysis of Kalnay et al. (1996).

gradual deepening of the late winter–spring mixed layer in the central North Pacific noted by Polovina et al. (1995) and Carton et al. (2008). This observed 20-m deepening into the cooler, fresher sub–mixed layer water has the effect of strengthening density compensation (the spice injection mechanism is discussed by Yeager and Large 2007). Carton et al. (2008) attribute the cause of mixed layer deepening to changes in the atmospheric forcing associated with the deepening of the Aleutian sea level pressure low after 1976. These changes led to strengthening of the midlatitude westerlies and the ocean surface heat loss in the North Pacific and hence the deepening of the mixed layer. The deepening of the mixed layer has opposite impacts on the width of CLs and BLs. It widens CLs by injecting saltier water from the mixed layer into fresher thermocline. In contrast, stronger atmospheric forcing and related deepening of the mixed layer normally destroys near-surface BLs by enhancing mixing. These mechanisms likely explain the narrowing of BLs and the widening of CLs in the North Pacific during recent decades (Figs. 7a,b).

Correlation analysis in Fig. 8 indicates that an association of the BL and CL width in the NP/BL and NP/CL boxes both seem to be associated with wind changes resulting from changes in the Aleutian surface pressure low. Widening of CLs in the NP/CL box is linked to anomalously strong westerly winds and a positive latent heat loss anomaly in the box (Fig. 8a). These two factors produce anomalous deepening of the mixed layer by amplifying wind stirring and convection. In the NP/CL

box, the observed CL width increases in phase with deepening of the mixed layer (see inlay in Fig. 8a). This in-phase relationship is in line with the spice injection mechanism of Yeager and Large (2007). In contrast to vertical widening of CLs in the NP/CL box, the BLs in the NP/BL box shrink when the local mixed layer deepens (Fig. 8a). A possible reason for this shrinking is the direct impact of wind stirring on BLs (as discussed in the previous paragraph). Another reason for this shrinking is changes in the surface freshwater flux itself. In fact, the anomalous wind pattern that produces westerly wind strengthening in the NP/BL box also includes anomalous northerly winds to the west of the Aleutian low. These anomalous northerly winds decrease moisture transport from the south and thus reduce the precipitation in the NP/BL box vital to maintaining the BL (Fig. 8b). Anomalously weak rainfall leads to shrinking of BLs in the NP/BL box. Shrinking of BLs occurs in phase with widening of CLs in the NP/CL box (just as in Figs. 7a,b).

Coherent variability of January–March CL width and MLD in the NP/CL box is evident in Fig. 9a. Besides the correspondence on decadal scales, both CL width (that is negative) and MLD display apparent out-of-phase interannual variations, so that widening of CLs occur in phase with deepening of the mixed layer. Variability of MLD in the box follows the variability of the winter Pacific decadal oscillation (PDO) index of Mantua et al. (1997) in line with previous findings of Deser et al. (1996) and Carton et al. (2008). Although in-phase changes of MLD and PDO do not hold during some years between 1980 and 1992, the time correlation between the two variables at zero lag evaluated during the entire period 1960–2007 is ~0.6 and exceeds the 99% level of zero correlation that is 0.4 (see also Fig. 7 in Carton et al. 2008). Correspondence of the mixed layer variability and the PDO suggests a link to variability of midlatitude westerly winds that, in turn, is linked to variability of the strength of the Aleutian low. In fact, this link is revealed by the time correlation analysis of the entire 1960–2007 record in Fig. 8a. Variability during particular interannual events also seems to be related to similar changes in winds. In particular, in winter of 1979 the westerly winds were weak in the southern part of the NP/CL box (Fig. 9b). As a result, the mixed layer was relatively shallow (~65 m deep, Fig. 9a) and CLs were missing and replaced by BLs produced by winter rainfall. By the next winter the westerly winds in the box are amplified because of the expansion of the Aleutian low (cf. areas within the 1000-hPa contour in Figs. 9b,c) and its southward shift. Enhanced mixing and convection due to stronger winds deepened the mixed layer down to 120 m, injected saltier mixed layer water into the thermocline, and produced 10-m-wide CLs (Fig. 9a).

d. Tropical oceans

The origin of persistent BLs in the tropics (Fig. 2) is ultimately linked to tropical precipitation. Direct correspondence of BL width with local precipitation is observed in the far western equatorial Pacific (Mignot et al. 2007). But in some tropical regions the lateral freshwater transport or three-dimensional circulation may also affect the BL width. In particular, the lateral transport of Amazon discharge water, freshwater transport from high rainfall, and river discharge areas along with local precipitation are all important for BL formation in the western tropical Atlantic (Pailler et al. 1999; Foltz et al. 2004; Mignot et al. 2007) as well as in the eastern equatorial Indian Ocean (Qu and Meyers 2005). In the western tropical Pacific at the eastern edge of the warm pool (where freshwater of the pool converges with saltier water to the east) BLs are affected by subduction of salty water in the convergence zone (Lukas and Lindstrom 1991).

Similar processes are involved at interannual time scales (Ando and McPhaden 1997; Cronin and McPhaden 2002). During La Niña when the Southern Oscillation index (SOI) is positive (SOI $>$ 0), tropical rainfall increases in the far western tropical Pacific and eastern tropical Indian Ocean (90°–160°E) by 1 mm day^{-1} or 20% of the local time mean rainfall (in response to a 10-unit decrease of the SOI) (Fig. 10b). This western increase is accompanied by decreased rainfall over the rest of the tropical Pacific while Amazonian and tropical Atlantic rainfall increase. As a result of these changes in rainfall, BL width in the western Pacific west of 160°E, which is normally 10–20 m, increases by 5 m (Figs. 10a,c). Thus, in the far western Pacific and eastern tropical Indian Ocean variations in BL width respond primarily to changes in surface freshwater flux. In the Atlantic sector excess discharge associated with the increases of rainfall over the Amazon does not result in an expected widening of BL (Fig. 10a). Possibly this lack of response may be because much of the Amazon discharge is transported in the Brazilian coastal zone.

The BL response to ENSO variability has local peak between the date line and 170°W (Fig. 10a). During El Niños the eastern edge of the Pacific warm pool expands into this zone accompanied by weakening upwelling and an eastward shift in the direction of near-surface currents to eastward (see, e.g., Fig. 2 in McPhaden 2004). The anomalous wind-driven downwelling creates conditions favorable for developing of BLs at the eastern edge of the warm pool via the Lukas and Lindstrom (1991) mechanism. Conversely, during La Niñas the warm pool contracts westward while strengthened easterly winds strengthen upwelling that, in turn, reduces (or shuts down) the subduction mechanism. So the negative correlation

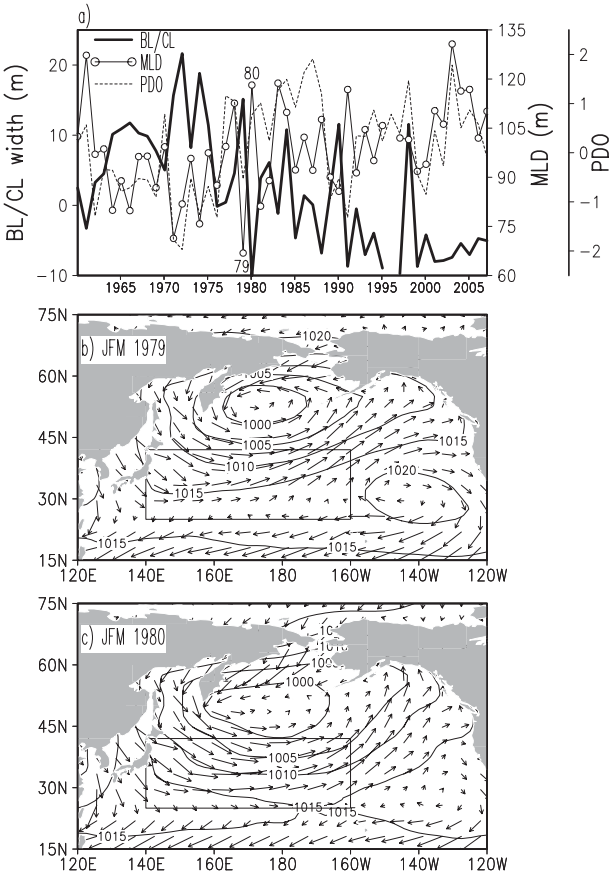

FIG. 9. (a) Times series of JFM BL/CL width and MLD averaged over the NP/CL box, and the PDO index. Data are shown for years with at least 10 measurements available for box averaging. JFM winds and mean sea level pressure (mbar) for years of (b) thin and (c) thick compensated layer. Atmospheric parameters are provided by the NCEP–NCAR reanalysis of Kalnay et al. (1996).

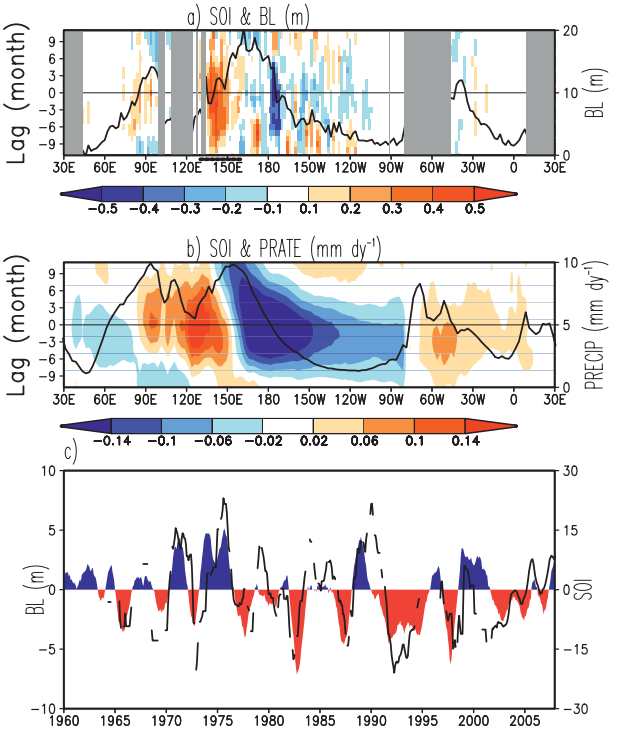

FIG. 10. Lag regression of SOI on 5°S–5°N averaged (a) anomalous barrier-layer width and (b) precipitation (Xie and Arkin 1997). Lag regressions show magnitude in response to 1-unit change of SOI. Solid lines in (a) and (b) are time mean BL width and precipitation. Longitude bands corresponding to land are shaded gray in (a). (c) Time series of annual running mean SOI (shaded) and anomalous BL width averaged over 5°S–5°N, 130°–160°E. Data are shown if more that 10 measurements are available for area averaging.

seen between 180° and 190°E in Fig. 10a reflects formation of BLs in the vicinity of the eastern edge of the warm pool during El Niños and the absence of these BLs during La Niñas.

4. Summary

This study examines subseasonal changes in barrier- and compensated-layer (BL and CL) width based on analysis of observed profiles of temperature and salinity covering the years 1960–2007. Because of data limitations we focus mainly on the Northern Hemisphere and tropics. The processes that regulate subseasonal variability of BL/CL width are similar to those that regulate their seasonal appearance: fluctuations in surface freshwater flux, Ekman pumping, and processes regulating mixed layer deepening. Thus, the spatial distribution of subseasonal variability reflects aspects of the subseasonal variability of these forcing terms. Companion studies (e.g., Foltz et al. 2004; Mignot et al. 2007) suggest that contribution of lateral freshwater advection is also important.

In the subtropics and midlatitudes during late winter–spring we find alternating regions of CLs and BLs in the seasonal climatology. The northern tropics of both the Pacific and Atlantic (the southern edge of the subtropical gyres) show broad regions of BLs where salty subtropical surface water formed farther north has subducted, advected equatorward, and affected the water properties of the winter mixed layer. Within the evaporative subtropical North Pacific and eastern North Atlantic we find CLs resulting from mixed layers with positive temperature stratification but negative salinity stratification. In the subtropics and midlatitudes variability occurs mostly during the local cold season when BLs and CLs are present. In the winter subpolar North Pacific a salinity-stratified BL exists that does not have a counterpart in the North Atlantic, while farther south along the Kuroshio Extension a CL exists. Much of the BL/CL width variability occurs at interannual periods, except in the North Pacific where longer-term changes

are detectable. The width of this BL varies from year to year by up to 60 m at some grid points, while CLs to the south experience variations of approximately half that. Longer-term variability results from a strengthening of the Aleutian pressure low during successive winters, thus strengthening the midlatitude westerly winds leading to deeper mixed layers, cooler SSTs, and a long-term increase in the width of the CL to the south. The same changes in meteorology that include strengthening of the Aleutian pressure low also lead to an increase in dry northerly winds which in turn cause a thinning of the area average northern BL width from ~40 m before 1980s to ~20 m afterward.

In the tropics the origin of persistent BLs is ultimately linked to precipitation. Precipitation in the tropics varies strongly interannually. During high precipitation years the mixed layer in this region shows capping fresh layers and thick BLs. In contrast, during low precipitation years mixed layer salinities increase and BL width decreases. In particular, in the western equatorial Pacific and eastern Indian Ocean between 90° and 160°E, the BL (which is normally 10–20 m wide in this area) thickens by 5 m during La Niña while during El Niño the BL thins by a similar amount in line with previous analysis of Ando and McPhaden (1997). During La Niña, rainfalls weaken in the tropical Pacific east of 160°E, which causes a minor decrease of BL width in the central and eastern tropical Pacific. But the BL width response to ENSO forcing amplifies between the date line and 170°W. This amplification is related to BL formation due to saltwater subduction near the eastern edge of the warm pool. This subduction strengthens during El Niño (when local equatorial upwelling is suppressed) and weakens during La Niña (when upwelling is restored).

Determining the basin-scale BL/CL structure tests the limits of the historical observing system. Further progress in understanding BL/CL variability and its role in air–sea interactions will likely require further exploration of models that provide reasonable simulations of observed variability.

Acknowledgments. We gratefully acknowledge the Ocean Climate Laboratory of the National Oceanographic Data Center/NOAA and the Argo Program upon whose data this work is based. Support for this research has been provided by the National Science Foundation (OCE0351319) and the NASA Ocean Programs. The authors appreciate comments and suggestions given by anonymous reviewers.

REFERENCES

Ando, K., and M. J. McPhaden, 1997: Variability of surface layer hydrography in the tropical Pacific Ocean. *J. Geophys. Res.,* **102,** 23 063–23 078.

Boyer, T. P., and Coauthors, 2006: *World Ocean Database 2005*. S. Levitus, Ed., NOAA Atlas NESDIS 60, 190 pp.

Carton, J. A., S. A. Grodsky, and H. Liu, 2008: Variability of the oceanic mixed layer, 1960–2004. *J. Climate,* **21,** 1029–1047.

Cronin, M. F., and M. J. McPhaden, 2002: Barrier layer formation during westerly wind bursts. *J. Geophys. Res.,* **107,** 8020, doi:10.1029/2001JC001171.

de Boyer Montégut, C., G. Madec, A. S. Fischer, A. Lazar, and D. Iudicone, 2004: Mixed layer depth over the global ocean: An examination of profile data and a profile-based climatology. *J. Geophys. Res.,* **109,** C12003, doi:10.1029/2004JC002378.

——, J. Mignot, A. Lazar, and S. Cravatte, 2007: Control of salinity on the mixed layer depth in the world ocean: 1. General description. *J. Geophys. Res.,* **112,** C06011, doi:10.1029/2006JC003953.

Deser, C., M. A. Alexander, and M. S. Timlin, 1996: Upper-ocean thermal variations in the North Pacific during 1970–1991. *J. Climate,* **9,** 1840–1855.

Endoh, T., H. Mitsudera, S.-P. Xie, and B. Qiu, 2004: Thermohaline structure in the subarctic North Pacific in a general circulation model. *J. Phys. Oceanogr.,* **34,** 360–371.

Ffield, A., 2007: Amazon and Orinoco River plumes and NBC rings: Bystanders or participants in hurricane events? *J. Climate,* **20,** 316–333.

Foltz, G. R., and M. J. McPhaden, 2009: Impact of barrier layer thickness on SST in the central tropical North Atlantic. *J. Climate,* **22,** 285–299.

——, S. A. Grodsky, J. A. Carton, and M. J. McPhaden, 2004: Seasonal salt budget of the northwestern tropical Atlantic Ocean along 38°W. *J. Geophys. Res.,* **109,** C03052, doi:10.1029/2003JC0021112004.

Grodsky, S. A., and J. A. Carton, 2003: Intertropical convergence zone in the South Atlantic and the equatorial cold tongue. *J. Climate,* **16,** 723–733.

Hurrell, J. W., 1995: Decadal trends in the North Atlantic oscillation—Regional temperatures and precipitation. *Science,* **269,** 676–679.

Kalnay, E., and Coauthors, 1996: The NCEP/NACR 40-Year Reanalysis Project. *Bull. Amer. Meteor. Soc.,* **77,** 437–471.

Kara, A. B., P. A. Rochford, and H. E. Hurlburt, 2000: Mixed layer depth variability and barrier layer formation over the North Pacific Ocean. *J. Geophys. Res.,* **105** (C7), 16 783–16 801.

Laurian, A., A. Lazar, and G. Reverdin, 2009: Generation mechanism of spiciness anomalies: An OGCM analysis in the North Atlantic subtropical gyre. *J. Phys. Oceanogr.,* **39,** 1003–1018.

Liu, W. T., 2002: Progress in scatterometer application. *J. Oceanogr.,* **58,** 121–136.

Lukas, R., and E. Lindstrom, 1991: The mixed layer of the western equatorial Pacific Ocean. *J. Geophys. Res.,* **96** (Suppl.), 3343–3357.

Maes, C., K. Ando, T. Delcroix, W. S. Kessler, M. J. McPhaden, and D. Roemmich, 2006: Observed correlation of surface salinity, temperature and barrier layer at the eastern edge of the western Pacific warm pool. *Geophys. Res. Lett.,* **33,** L06601, doi:10.1029/2005GL024772.

Mantua, N. J., S. R. Hare, Y. Zhang, J. M. Wallace, and R. C. Francis, 1997: A Pacific interdecadal climate oscillation with impacts on salmon production. *Bull. Amer. Meteor. Soc.,* **78,** 1069–1079.

McPhaden, M. J., 2004: Evolution of the 2002/03 El Niño. *Bull. Amer. Meteor. Soc.,* **85,** 677–695.

Mignot, J., C. de Boyer Montégut, A. Lazar, and S. Cravatte, 2007: Control of salinity on the mixed layer depth in the world

ocean: 2. Tropical areas. *J. Geophys. Res.,* **112,** C10010, doi:10.1029/2006JC003954.

Pailler, K., B. Bourlès, and Y. Gouriou, 1999: The barrier layer in the western tropical Atlantic Ocean. *Geophys. Res. Lett.,* **26,** 2069–2072.

Polovina, J. J., G. T. Mitchum, and G. T. Evans, 1995: Decadal and basin-scale variation in MLD and the impact on biological production in the central and North Pacific, 1960-88. *Deep-Sea Res.,* **42,** 1701–1716.

Qu, T., and G. Meyers, 2005: Seasonal variation of barrier layer in the southeastern tropical Indian Ocean. *J. Geophys. Res.,* **110,** C11003, doi:10.1029/2004JC002816.

Ruddick, B., 1983: A practical indicator of the stability of the water column to double-diffusive activity. *Deep-Sea Res.,* **30,** 1105–1107.

Sato, K., T. Suga, and K. Hanawa, 2004: Barrier layer in the North Pacific subtropical gyre. *Geophys. Res. Lett.,* **31,** L05301, doi:10.1029/2003GL018590.

Sprintall, J., and M. Tomczak, 1992: Evidence of the barrier layer in the surface layer of the tropics. *J. Geophys. Res.,* **97** (C5), 7305–7316.

——, and ——, 1993: On the formation of central water and thermocline ventilation in the Southern Hemisphere. *Deep Sea Res. I,* **40,** 827–848.

Stommel, H., and K. N. Fedorov, 1967: Small-scale structure in temperature and salinity near Timor and Mindanao. *Tellus,* **19,** 306–325.

Thadathil, P., and Coauthors, 2008: Seasonal variability of the observed barrier layer in the Arabian Sea. *J. Phys. Oceanogr.,* **38,** 624–638.

Tomczak, M., and J. S. Godfrey, 1994: *Regional Oceanography: An Introduction*. Pergamon Press, 422 pp.

Ueno, H., and I. Yasuda, 2000: Distribution and formation of the mesothermal structure (temperature inversions) in the North Pacific subarctic region. *J. Geophys. Res.,* **105** (C7), 16 885–16 897.

Waliser, D. E., 1996: Formation and limiting mechanisms for very high sea surface temperature: Linking the dynamics and the thermodynamics. *J. Climate,* **9,** 161–188.

Weller, R. A., and A. J. Plueddemann, 1996: Observations of the vertical structure of the oceanic boundary layer. *J. Geophys. Res.,* **101,** 8789–8806.

Xie, P., and P. A. Arkin, 1997: Global precipitation: A 17-year monthly analysis based on gauge observations, satellite estimates, and numerical model outputs. *Bull. Amer. Meteor. Soc.,* **78,** 2539–2558.

Yeager, S. G., and W. G. Large, 2007: Observational evidence of winter spice injection. *J. Phys. Oceanogr.,* **37,** 2895–2919.